

## **RANKING THE BUILDINGS OVER A DEVELOPED LARGE GEOGRAPHIC AREA ACCORDING TO THEIR EXPOSURE TO THE LANDSLIDE HAZARD.**

**Paolino DI FELICE**

*University of L'Aquila, Department of Industrial and Information Engineering and Economics, Italy*  
[paolino.difelice@univaq.it](mailto:paolino.difelice@univaq.it)

**Andrea BUFALINO**

*University of L'Aquila, Department of Industrial and Information Engineering and Economics, Italy*

**Eugenio CAROCCI**

*University of L'Aquila, Department of Industrial and Information Engineering and Economics, Italy*

**Lorenzo DI GIUSEPPE**

*University of L'Aquila, Department of Industrial and Information Engineering and Economics, Italy*

**Matteo GENTILE**

*University of L'Aquila, Department of Industrial and Information Engineering and Economics, Italy*

**Alessandro RANALLI**

*University of L'Aquila, Department of Industrial and Information Engineering and Economics, Italy*

**Andrea SALINI**

*University of L'Aquila, Department of Industrial and Information Engineering and Economics, Italy*

---

### **Abstract**

In this paper, we focus on public buildings. They represent a relevant category of elements because of their intrinsic economic value and because their damage may cause human casualties as well. If the survey covers developed, large geographic areas, the number of buildings potentially at risk exposed is very high. Such numbers make the use of the available methods of building risk assessment highly time-consuming and, hence, inapplicable in the reality. To mitigate such an issue, we introduce a method that takes as input all the buildings standing over the study area and outputs a ranking about them according to their degree of exposure to the landslide hazard. The practitioners in mitigation can extract from the ranking the top-N buildings to look at. Then, they need to carry out the detailed risk assessment only for the buildings on the short list. This way the overall processing time required for the computation of the vulnerability, and hence of the risk, is reduced dramatically. The ranking method has been tested to assess the exposure to the landslide hazard of the buildings hosting public schools in the Abruzzo Region (center of Italy), a large area (11,000 km<sup>2</sup>) with 1,330,000 inhabitants. The results obtained from the case study show that the top-N buildings to look at are a very small fraction of the total number of buildings in the region.

**Keywords:** *Landslide, Hazard, Element at risk, Building ranking, Geographical database, GIS.*

---

## 1. PRELIMINARY CONSIDERATIONS

Landslides constitute one of the most important natural hazards in many countries all over the world, (Brabb and Harrod, 1989). This is the case of Italy where landslides are widespread and result in considerable damage and fatalities every year, (Guzzetti, Stark, and Salvati, 2005), (Trigila et al., 2010). According to the outcome of a very recent study carried out by Jaedicke et al. (2014), "Italy has the highest number of people exposed to landslide hazard among the European countries."

Landslides, as a natural process, present no threat to themselves. For this to happen there must be an interaction with the so-called *elements at risk*, namely, humans and infrastructures (e.g. buildings, roads, railways, etc.). The evaluation of the side effects (casualties and/or loss of assets) of landslide, as a consequence of a natural trigger (a trigger can be the effect of precipitation, snow melt, seismic activity or human activities such as excavation), is usually called *risk assessment* (Jaedicke et al., 2014). In mathematical terms, the risk may be defined as in (Varnes et al, 1984):

$$risk = Hazard \times Elements\ at\ risk \times Vulnerability$$

where *vulnerability* is the degree of loss of an element at risk. It is expressed on a scale from 0 (no damage) to 1 (total loss).

There are many publications about landslide risk assessment (e.g. Jaedicke et al., 2014; Erener and Düzgün, 2013; Varazanashvili et al., 2012; Dai et al., 2002) and vulnerability (e.g. Fuchs et al. 2012; Fuchs et al. 2011; Galli and Guzzetti, 2007); while less attention has been devoted to the issue of making available to the community a method for ranking the elements at risk exposed over a developed, large geographic area. Often, surrogates of the actual elements inside a landslide exposed area are used. For instance, Varazanashvili et al. (2012) adopt the Gross Domestic Product (applied to population) as an indicator of the elements at risk for a study at the national level (the Republic of Georgia), while Jaedicke et al. (2014) consider the total number of people living in landslide exposed areas within Europe.

In this paper, we focus on public buildings. They are a relevant category of elements exposed to the landslide hazard because of their intrinsic economic value and because their damage may cause human casualties as well. With respect to buildings, the approach mainly adopted so far has been to restrict the geographic area of interest to a few dozens of square kilometers up to some hundreds. For instance, the territory taken into account in (Galli and Guzzetti, 2007) extends for about 80 km<sup>2</sup> (the Collazzone area, Umbria, Italy), while in (Erener and Düzgün, 2013) authors refer to an area of about 330km<sup>2</sup> (the Kumluca watershed, northern Turkey).

If the survey covers developed, large geographic areas (for instance Jaedicke et al., 2014, "perform a first-pass analysis of landslide hazard at the European scale"), the number of buildings potentially involved is very high. For example, in Italy there are 72,355 schools located in 43,643 distinct buildings, while the total number of public buildings is much bigger. Such numbers make the use of the available methods of building risk assessment highly time-consuming and, hence, inapplicable in the reality. To mitigate such an issue, we introduce a method that takes as input all the buildings standing over a developed, large territory and outputs a ranking about them according to their degree of exposure to the landslide hazard. The exposure we refer to in the paper is called "spatial" exposure in (SafeLand, 2011). We compute the (spatial) buildings' exposure with a formula that takes into account the landslides "close" to them and their "size".

Once the appropriate ranking is provided, the officials and practitioners in mitigation can have a short list of targets for them to look at (namely, the top-N buildings with a value of the exposure above a given threshold). Then, they need to carry out the detailed risk assessment only for the buildings on the short list. This way the overall processing time required for the

computation of the vulnerability, and hence of the risk, is reduced dramatically. The most severe cause that dilates the time needed for estimates concerns the gathering of the input data necessary to calculate the building vulnerability (namely: age, number of floors, footprint area, state of preservation, materials, etc). Moreover, in the literature it is widely reported that the available datasets at the regional and state level are often not up to date, neither complete, e.g. (Mazzorana et al., 2014), (Erener and Düzgün, 2013), (Varazanashvili et al., 2012).

The ranking method has been tested to assess the exposure to the landslide hazard of the buildings hosting public schools in the Abruzzo Region (center of Italy), a large area (11,000 km<sup>2</sup>) with 1,330,000 inhabitants. The results obtained from the case study show that the top-N targets to take care of are a very small fraction of the total number of buildings exposed to the landslide hazard.

The ranking problem has its origins in the domain of Information Retrieval. While methods to rank buildings have been proposed in recent years. Methods to build fire risk ranking of buildings, for instance, have already appeared in the literature, e.g. (Liu et al., 2009). Another scheme for ranking buildings in a given geographic area according to their environmental performances may be found in (Peri and Rizzo, 2012). As far as we know, methods for ranking the buildings present over a developed, large territory, according to the degree of exposure to the landslide hazard, have not been proposed yet.

The remainder of the paper is structured as follows: Section 2 introduces the basic notations used throughout the paper and it presents the method to tag each building with a value of the exposure to the landslide hazard and a high-level algorithm that implements. It reports about the case study we carried out to test the proposed method and it gives an overview of the Geographical DataBase (Geo-DB in the following) used to implement the theory and collects the results of the experiments. Section 3 reports the results of those experiments and discusses them. Conclusions and further work are outlined in Section 4.

## 2. MATERIALS AND METHODS

### 2.1. Notations

Hereafter we use the following notations:

$\mathcal{GeoArea}$  is a portion of land globally affected by a hazard caused, for example, by a prolonged and heavy period of rainfall.  $\mathcal{GeoArea}$  may coincide with a municipality, a province, a region, a country or an entire continent (a recent example of a study about the landslide hazard at the European scale may be found in Jaedicke et al., 2014).  $\mathcal{GeoArea}$  is defined by the pair  $\langle description, geometry \rangle$  of its boundary, where *description* is a string;

$\mathcal{DZ} = \{z_k (k=1, 2, \dots) \mid z_k \text{ is a danger zone}\}$ . The elements in  $\mathcal{DZ}$  make a full partition of  $\mathcal{GeoArea}$ . In other words, knowing set  $\mathcal{DZ}$  for a given area is equivalent to have built a map like that prepared by Guzzetti et al., (2006) for the Collazzone area (central Umbria, Italy). According to the existing literature, e.g. (Guzzetti et al., 2006) and (Fell et al., 2008)), by *danger zone* we mean a portion of land characterized by a set of ground conditions. Brabb (1984) introduced the term *susceptibility* to denote the propensity of an area to generate landslides. The generic element of  $\mathcal{DZ}$  (i.e.,  $z_k$ ) is defined by the tuple  $\langle ID, S_{z_k}, boundary, area \rangle$ , being ID an identifying code.  $S_{z_k}$  is a numerical value that quantifies the (*spatial*) *probability* that  $z_k$  produces landslides. Assessing and mapping landslide susceptibility has been a relevant issue, e.g. (Magliulo et al., 2009). The meaning of *boundary* and *area* is obvious.  $Card(\mathcal{DZ})$  denotes the cardinality of the set  $\mathcal{DZ}$ , i.e., the number of elements in the set;

$\mathcal{B} = \{b_i (i=1, 2, \dots) \mid b_i \text{ denotes a building whose boundary is contained in the boundary of } \mathcal{G}\mathcal{E}\mathcal{O}\mathcal{A}\mathcal{R}\mathcal{Z}\mathcal{A}\}$ . We do not care about either the height or the number of floors of  $b_i$ . Its outline on the ground is certainly interesting, but experience teaches that this data is rarely available, while the geographic position, expressed by a pair of coordinates, is often known.  $Exp\_b_i$  is a positive numeric value denoting the degree of (spatial) exposure of  $b_i$  to the landslide hazard caused by *all* the  $z_k$  in  $\mathcal{D}\mathcal{Z}$ ; while  $Exp\_b_{i,k}$  denotes the degree of exposure of  $b_i$  to the hazard caused by zone  $z_k$ . Each building in  $\mathcal{B}$  is defined by the tuple  $\langle ID, description, position, Exp\_b_i \rangle$ , being ID an identifying code.  $Card(\mathcal{B})$  denotes the cardinality of set  $\mathcal{B}$ ;

$\mathcal{D}\mathcal{Z}_i = \{z_k \mid z_k \in \mathcal{D}\mathcal{Z} \text{ and } (\text{boundary of } z_k \cap \text{buffer of radius } \rho \text{ centered on } b_i) \neq \emptyset\}$ .  $\rho$  denotes the distance from building  $b_i$  beyond which danger zones do not contribute significantly to increasing the value of  $Exp\_b_i$ . This conjecture is inspired by the Tobler's first law of geography (Tobler, 1970): "Everything is related to everything else, but near things are more related than distant things."  $Card(\mathcal{D}\mathcal{Z}_i)$  denotes the cardinality of set  $\mathcal{D}\mathcal{Z}_i$ .

Figure 1 depicts the previous definitions.

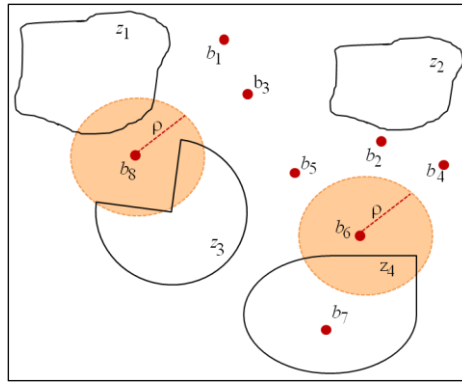


**Figure 1.** A scene about a  $\mathcal{G}\mathcal{E}\mathcal{O}\mathcal{A}\mathcal{R}\mathcal{Z}\mathcal{A}$  (the rectangle), buildings and danger zones.  $\mathcal{B}=\{b_1, \dots, b_8\}$ ,  $\mathcal{D}\mathcal{Z}=\{z_1, \dots, z_4\}$ ,  $\mathcal{D}\mathcal{Z}_6=\{z_4\}$  and  $\mathcal{D}\mathcal{Z}_8=\{z_1, z_3\}$ . Buildings are depicted by their centroid (the small circle).

## 2.2. The method

Our method takes as input the sets  $\mathcal{B}$  and  $\mathcal{D}\mathcal{Z}$  and outputs a ranking about the buildings in the  $\mathcal{G}\mathcal{E}\mathcal{O}\mathcal{A}\mathcal{R}\mathcal{Z}\mathcal{A}$ , according to their degree of exposure to the landslide hazard. The value of  $Exp\_b_i$  is determined by three factors: the distance of building  $b_i$  from the neighbouring danger zones, the "size" of those zones, and the spatial probability ( $Sz_k$ ) that they produce a landslide. Hereafter, we discuss the role of these three factors and introduce the equations to compute the ranking.

### 2.2.1 The role of the distance

The method we are going to introduce for the computation of the value of  $Exp\_b_i$  is based on the conjecture that *only* the danger zones that are close to building  $b_i$  might pose a threat to its safety. Let us examine the implications of this conjecture with respect to the scene of Figure 2, which shows a generic building ( $b_i$ ), the boundary of danger zones close to it and the distance of those zones from the building. The implications are listed hereafter: a)  $Exp\_b_{i,3} = Exp\_b_{i,7}$  being  $d_3 = d_7$  and the size of  $z_3$  is equal to the size of  $z_7$  (i.e., two zones of the same size, located at the same distance from a building induce on it the same degree of exposure to the landslide hazard); b)  $Exp\_b_{i,5} > Exp\_b_{i,1}$  being  $d_5 < d_1$  and the size of  $z_5$  is equal to the size of  $z_1$  (i.e., two zones of the same size, located at different distances from a building induce on it a degree of exposure to the landslide hazard decreasing with the distance); c) danger zones

far away from a building do not represent an hazard for it. To conclude, and again referring to the scene of Figure 2, it is correct that the computation method assigns the maximum weight to zone  $z_6$  because it contains  $b_i$  and decreasing weights to the zones  $z_4$ ,  $z_3$ ,  $z_7$ ,  $z_5$ ,  $z_2$ , and  $z_1$ .

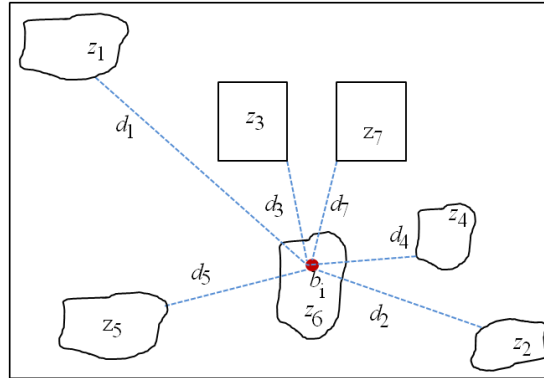


**Figure 2.** A building ( $b_i$ ) and the surrounding danger zones ( $z_1$ ,  $z_2$ ,  $z_3$ ,  $z_4$ ,  $z_5$ ,  $z_6$ , and  $z_7$ ).

About the choice of the decay law, we can say that in our study this is not a critical issue because the goal of the proposed method is to draw up a ranking about the buildings from which the officials and practitioners in mitigation can identify the top-N buildings to take care of. Vice versa, the absolute value of the exposure of the buildings is negligible. The basic requirement to be satisfied is that the chosen law must ensure that the value of the exposure (i.e.,  $Exp_{b_i,k}$ ) tends to zero rapidly as the distance between the building and the danger zone increases. Among the available alternatives, we took into account the *cube* law. A cue that suggests not to go beyond the cubic law comes from the context of the evaluation of the spatial rainfall distribution using the *inverse distance weighting* method, e.g. (Di Felice et al., 2014).

Eq.1 and Eq.2 allow the computation of the exposure of building  $b_i$ :

$$Exp_{b_i} = \sum_{k=1}^n Exp_{b_i,k} \quad (1)$$

and

$$Exp_{b_i,k}(d) = Size \times S_{z_k} \times \begin{cases} 1 & \text{if } b_i \text{ is contained in } z_k \text{ or } d \leq d_0 \\ \left(\frac{d_0}{d}\right)^p & \text{otherwise} \end{cases} \quad (2)$$

where:

- $n$  is equal to  $card(\mathcal{DZ}_i)$ ;
- $p = 3$ ;
- $d_0$  is the radius of the circle centered on the centroid of building  $b_i$ , the circle that approximates the area of  $b_i$ . In the literature very often the centroid of a geometric entity is adopted as an abstraction of the whole object, e.g. (Di Felice, 2015) and (Photis, 2012). The need of introducing a buffer stems from the awareness that is too coarse approximate a school building with its centroid;
- $d$  denotes the minimum distance between  $b_i$  and the boundary of zone  $z_k$ . The spatial relationship between  $b_i$  and a generic  $z_k$  is one of the three shown in Figure 3; namely: (i) the centroid of  $b_i$  falls inside the boundary of  $z_k$ ; (ii) the buffer of radius  $d_0$  centered on  $b_i$  intersects the boundary of  $z_k$ ; (iii)  $z_k$  is at minimum distance  $d > d_0$  from  $z_k$ ;

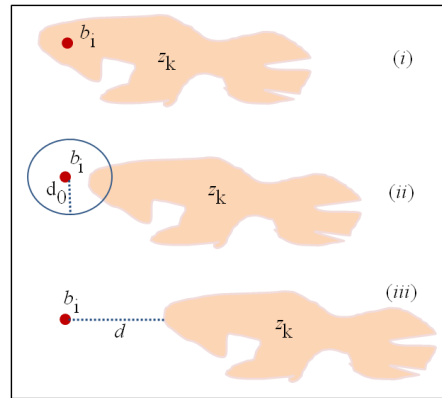


**Figure 3.** The three realizable spatial relationships between a building ( $b_i$ ) and a zone ( $z_k$ ).

The term  $(d_0/d)$  of Eq.2 plays two roles:

- it ensures continuity of the values of parameter  $Exp\_b_{i,k}$ . In fact, if the danger zone  $z_k$  is located at a distance  $d=d_0$  from the centroid of building  $b_i$ , then  $Exp\_b_{i,k} = S_{z_k} \times Size$ ;
- it represents the decay factor of the value of term  $Exp\_b_{i,k}$  as the minimum distance between the centroid of  $b_i$  and  $z_k$  increases. The value of  $p$  determines the rate of decay of term  $(d_0/d)$  and, hence, the weight of the contribution given by the danger zone  $z_k$  to the value of the exposure.

### 2.2.2 The role of the size of the danger zones

In Eq.2 the factor *Size* takes into account the area of  $z_k$ . In this way the intelligence of the method that computes the value of the exposure increases, as explained below. Let us refer to the three scenes of Figure 4 under the double assumption that  $d_1=d_2=d_3$  and  $S_{z_1}=S_{z_2}=S_{z_3}$ . If factor *Size* is removed from Eq.2, then such an equation can not distinguish numerically those three scenes anymore (in fact, it would return  $Exp\_b_{i,1} = Exp\_b_{j,2} = Exp\_b_{k,3}$ ), as it, vice versa, does (in fact, it returns  $Exp\_b_{i,1} < Exp\_b_{j,2} < Exp\_b_{k,3}$ ).

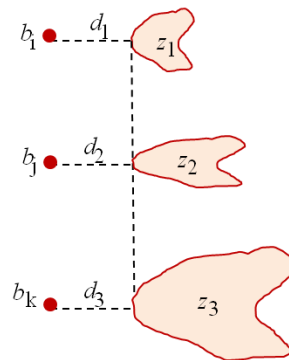


**Figure 4.** Three scenes, each involving a building and a danger zone. By hypothesis, in the three cases the distance building-zone is constant,  $S_{z_1}=S_{z_2}=S_{z_3}$ , while  $Size_1 < Size_2 < Size_3$ .

By taking into account the size of the danger zones, it is possible, moreover, to model in a proper manner the two configurations shown in Figure 5. They involve two different buildings ( $b_i$  and  $b_j$ ) with only one zone ( $z_1$ ) in the vicinity, in the scene to the left, and three danger zones ( $z_2$ ,  $z_3$ , and  $z_4$ ), in the scene to the right. In formulas, the two scenes are described by the following analytical conditions (where  $i = 2, 3, 4$ ):

- area of  $z_1 \gg$  area of  $z_i$ ;
- $d_1 = d_i$ ; (i.e., the value of the minimum distances is the same in the four cases);
- $S_{z_1} = S_{z_i}$  (i.e., the four zones have the same probability to produce landslides).



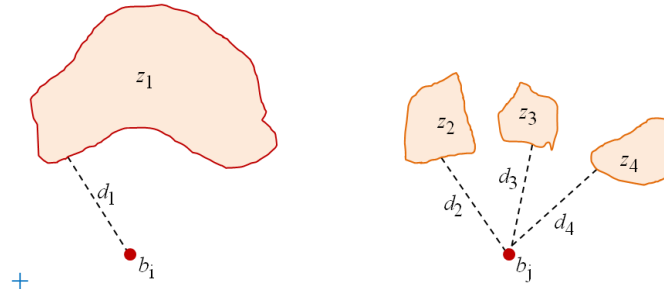


**Figure 5.** Two scenes involving two different buildings and a different number of danger zones in the surrounding. By hypothesis, in the two cases the zones have the same value of  $Sz_k$ , but very different area.

By applying Eq.2 (without the term *Size*) to the two scenes of Figure 5, it follows that:

$Exp_{b_1} = 3 \times Exp_{b_2}$ . This result is not satisfactory, vice versa, what we should expect is that  $Exp_{b_1} > Exp_{b_2}$ , because area of  $z_1 > (\text{area of } z_2) + (\text{area of } z_3) + (\text{area of } z_4)$ .

In fact, in the event of a movement of the four landslide zones of Figure 6, the amount of debris that could invest the two buildings is greater in the former case than in the second one. Obviously, this statement is correct if the direction of motion of the debris of the four zones is the same and it is against the two buildings. In summary, the *Size* term ensures that things go as we understand intuitively they should go.

Eq.3 defines the *Size* term for a generic danger zone. The value of *Size* is close to zero for very small danger zones, while it is greater than 1 for *all* zones with the area above the value of the average area. *Size* reaches high values for very large zones.

$$Size = \frac{\text{area of } z_k}{\text{the average of the values of all the areas of zones in SZ}} \quad (3)$$

The idea of giving a significant weight to large areas is based on field studies. For instance, Galli and Guzzetti (2007), in a study with regard to the Umbria region, central Italy, conclude that the area of the landslides affecting buildings is widely variable (they report values that range from 258m<sup>2</sup> to 165,237m<sup>2</sup>). Moreover, they found that landslides smaller than 2,000m<sup>2</sup> resulted in aesthetic to functional damage of buildings, whereas landslides larger than 10,000m<sup>2</sup> produced functional to structural or total damage of buildings. More specifically, they found that landslides whose area is around 160,000m<sup>2</sup> always produce total damage of buildings.

In conclusion, Eq.2 formalizes the guess that the top positions in the ranking to be returned have to concern the buildings located inside danger zones of a big area. In fact, when such a double circumstance comes true, Eq.2 simplifies to  $Exp_{b_{i,k}} = Size \times Sz_k$ ; that is, exponent  $p$  no longer plays a role since the distance between the building and  $z_k$  is zero, while the terms  $Sz_k$  and *Size* determine the value of  $Exp_{b_{i,k}}$ . About the zones close to  $b_i$ , the threat that they might pose to  $b_i$  diminishes rapidly with the distance (see Eq.2).

### 2.3 An algorithm that computes the building exposure

Algorithm *ComputeBuildingExposure* implements Eq.1, Eq.2 and Eq.3.

Algorithm **ComputeBuildingExposure**

INPUT:

$b_i; \mathcal{DZ}_i; d_0; p; avgArea;$   
**OUTPUT:**  
 $Exp\_b_i$   
**METHOD:**  
 $Exp\_b_i \leftarrow 0;$   
**FOREACH**  $z_k$  **in**  $\mathcal{DZ}_i$   
     $Exp\_b_{i,k} \leftarrow (area\ of\ z_k / avgArea) \times Sz_k;$   
    **IF** ( $b_i$  is not contained in  $z_k$ ) **THEN**  
         $distance \leftarrow$  minimum distance between  $b_i$  and  $z_k$ ;  
         $Exp\_b_{i,k} \leftarrow Exp\_b_{i,k} \times (d_0 / distance)^p;$   
    **ENDIF**;  
 $Exp\_b_i \leftarrow Exp\_b_i + Exp\_b_{i,k};$   
**RETURN**  $Exp\_b_i$ ;

$avgArea$  denotes the value of the average area among *all* the danger zones in  $\mathcal{DZ}$ . The complexity of algorithm *ComputeBuildingExposure* is  $O(\text{card}(\mathcal{DZ}_i))$ , under the assumption that the computation of the distance between  $b_i$  and  $z_k$  costs  $O(1)$  and  $O(1)$  is also the cost of assessing whether  $b_i$  is contained in  $z_k$ . To build the global ranking, it is necessary to repeat the execution of algorithm *ComputeBuildingExposure* for all the buildings in  $\mathcal{GeoArea}$ ; hence, the overall cost is  $O(\text{card}(\mathcal{B}) \times \text{card}(\mathcal{DZ}_i))$ . Moreover,  $O(\text{card}(\mathcal{DZ}))$  is the cost of the pre-computation devoted to calculating the value of  $avgArea$ .

## 2.4. The case study

### 2.4.1 Input datasets

$\mathcal{GeoArea}$

$\mathcal{GeoArea}$  coincides with the boundary of the Abruzzo region (Figure 6). An area of about 11,000 km<sup>2</sup>, structured as four provinces, 305 municipalities and a population of about 1,330,000. We downloaded the shapefile about Abruzzo from the ISTAT website (<http://www.istat.it/it/archivio/124086>).

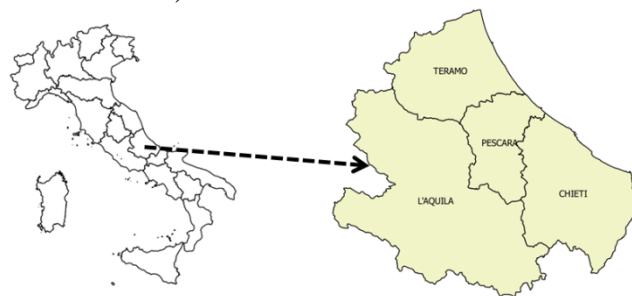


**Figure 6.** The  $\mathcal{GeoArea}$  of the case study.

Set  $\mathcal{B}$

It concerns a category of public buildings of particular social interest: the school buildings of the Abruzzo region. We downloaded the dataset (in the shapefile format) about the Italian primary and secondary schools from the website of the National Geoportal of Italy (<http://www.pcn.minambiente.it/GN/>). The dataset consists of 72,355 records of which 1,919 relate to schools that fall in the Abruzzo region. Those 1,919 schools are located inside 1,140 distinct buildings. The geographic position of each building is expressed by a pair of coordinates.



## Set $\mathcal{DZ}$

For the Abruzzo region, it is not available a dataset with the characteristics of set  $\mathcal{DZ}$ . What we have found was a shapefile about the *landslide inventory* of the region (a *landslide inventory* is a detailed register of the distribution and characteristics of past landslides; Hervás, 2013. Landslide inventories are often used by scholars. For instance, Mandal (2013) used landslide inventory statistics to investigate the relationship between rainfall and landslip events.). The limit of this dataset is that it does not achieve a complete partition of the region. This (real) dataset coincides with the "theoretical one" by setting  $S_{zk} = 0$  for the portions of land not surveyed.

Within the landslide inventory, landslides are classified according to the type of movement, the estimated age, the state of activity, the depth of failure surface, and the velocity. The categories of landslides making part of the inventory are fall/topple, rotational/transational slide, slow earth flow, rapid debris flow, sinkhole, complex landslide. Moreover, landslides are classified as *active*, *quiescent/dormant*, and *inactive*.

The elements contained in the Abruzzo landslide inventory are grouped into three susceptibility *classes* called *S1* (*low* susceptibility), *S2* (*high* susceptibility), and *S3* (*very high* susceptibility). This is in line with the following statement taken from (Fell, et al., 2008): "It should be recognized that the study area may be susceptible to more than one type of landslide and may have a different degree of susceptibility for each of these." Overall, the inventory is composed of 4,425 elements in *S1*, 8,886 elements in *S2* and 3,959 elements in *S3*. With few exceptions, it can be said the following: *S3* includes *active* landslides, *quiescent* landslides are in *S2*, while *inactive* landslides are in *S1*. All the areas about badlands are part of class *S3*. Figure 7 shows a map that overlays the three datasets about the Abruzzo landslide inventory.

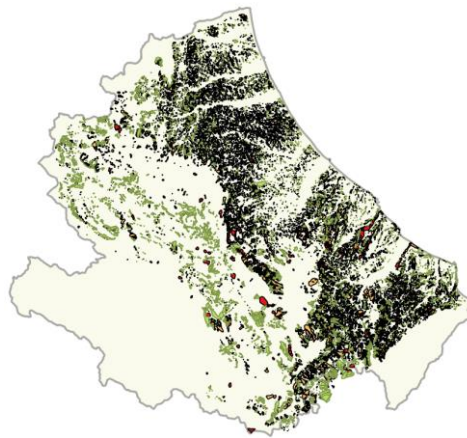


**Figure 7.** A (QGIS) map about the danger zones part of the Abruzzo landslide inventory. Red polygons are *S3* zones, orange polygons are *S2* zones, green polygons are *S1* zones.

The area of the landslides in  $\mathcal{DZ}$  ranges from 161 m<sup>2</sup> to 9,847,888 m<sup>2</sup>. The average area measures 93,887 m<sup>2</sup>.

## Values of the parameters used in the experiments

The ground position of the elements in  $\mathcal{B}$  is described by a point denoting their centroid, while the real extension of the school buildings is unknown. About the average size of school buildings, it was decided to put  $d_0=50\text{m}$  following feedback from the field.

As just said, the case study partitions the set of danger zones  $\mathcal{DZ}$  into three classes each characterized by a single value for  $S_{zk}$  for all the  $z_k$  belonging to it. This is a simplification of the general case (Sec.2.1), which does not exclude that each  $z_k$  has a specific value for  $S_{zk}$ . In order to carry out the experiments, we have associated to the zones in the aforementioned

three classes the values 25, 50 and 100, respectively. Obviously those values may be changed, but the following constraint must be fulfilled: the value of  $S_{zk}$  must be positive (remember that it expresses a probability value) and such that  $S_{zk}(\text{class } S1) < S_{zk}(\text{class } S2) < S_{zk}(\text{class } S3)$ .

## 2.5. The Geographical DataBase

We implemented a PostgreSQL/PostGIS Geo-DB to code the *ComputeBuildingExposure* algorithm (i.e., Eq.1, Eq.2, and Eq.3), and also to store the records of the input shapefiles and the results of the experiments to be carried out. The relevance of Geo-DBs as a useful tool for the management of the hydrological hazard is well-known in the literature, see for instance (Blahut, et al., 2012), (Rawat et al., 2012).

Algorithm *ComputeBuildingExposure* has been implemented as User Defined Functions (UDFs) in the PL/pgSQL language, making use of PostGIS's functionality. Consequently, all the experiments were carried out by running SQL queries against the database. Di Felice et al. (2014) emphasize the utility and effectiveness of UDFs on top of a Geo-DB.

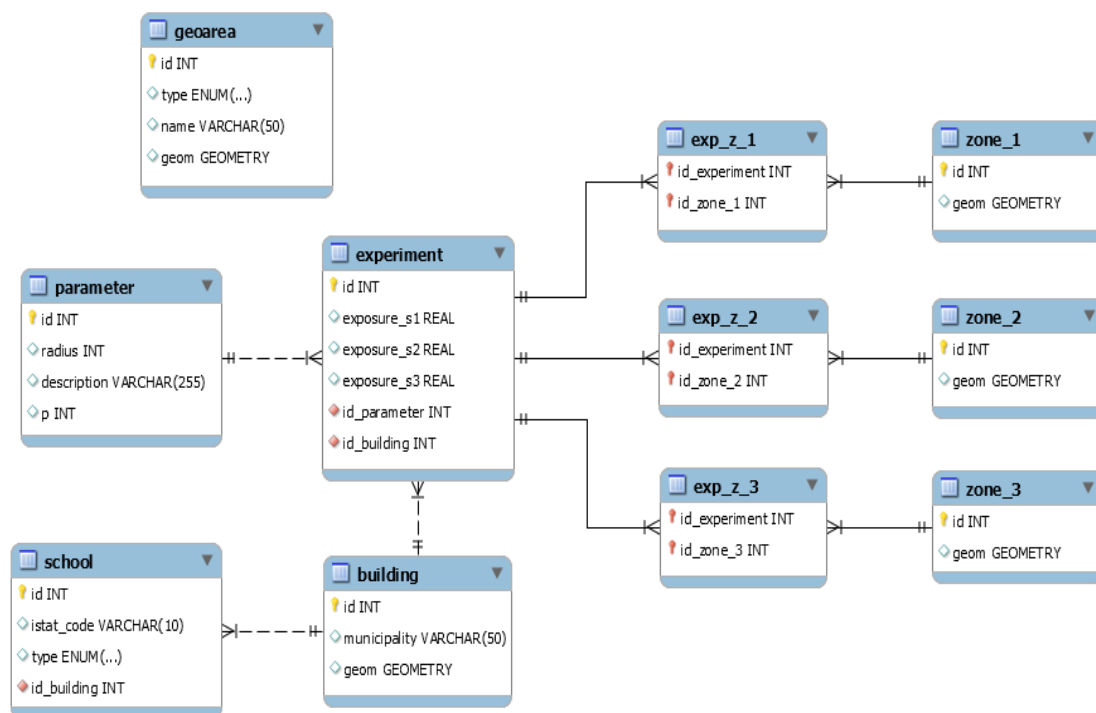


Figure 8. A graphical representation of the Geo-DB.

Figure 8 shows the structure of the Geo-DB. Tables **geoarea**, **building**, **zone\_1**, **zone\_2**, and **zone\_3** store data about sets  $\mathcal{GeoArea}$ ,  $\mathcal{B}$ , and  $\mathcal{DZ}$ , respectively (Sec.2.1). Table **school** stores data about the Abruzzo's schools and the identifier of the building they are contained in. Table **parameter** stores different values of  $\rho$  (attribute **radius**) and  $p$ . Table **experiment** collects the results of the experiments to be carried out. In detail, the attributes **exposure\_s1**, **exposure\_s2**, and **exposure\_s3** store the value of parameter  $Exp_{b_i}$  (Eq.1) determined by the danger zones of classes  $S1$ ,  $S2$  and  $S3$ , respectively, for a specific building (**id\_building**), for a particular value of the radius (**id\_parameter**),

and for a value of exponent  $p$ . Tables **exp\_z1**, **exp\_z2** and **exp\_z3** link a building (**id\_building**) to the nearby danger zones (set  $\mathcal{DZ}_i$ , Sec.2.1).

### 3. RESULTS AND DISCUSSION

By making use of the implemented Geo-DB and the UDFs coded on top of it, it was possible to carry out a high number of experiments, by varying  $\rho$  (500m, 1,000m, 10,000m). This section collects the results of the experiments and comments on them.

Table 1 assembles the top-20 values of the exposure for  $\rho$  equal to 500m, 1,000m and 10,000m. As can be seen, the ranking positions of the buildings in the study area remain unchanged, so it can be stated that the proposed method is *stable*. As said in Sec.2.2, the danger zones far away from a building do not induce any potential danger on it. The reason why we tested  $\rho=10,000$ m was to give an experimental proof that the filter implemented by Eq.2 produces that expected effect.

**Table 1.** The ranking of the top-20 buildings in the study area for  $\rho=500$ m,  $\rho=1,000$ m,  $\rho=10,000$ m.

$b_i$	$\rho$		
	500m	1,000m	10,000m
$Exp_{b_i}$	$Exp_{b_i}$	$Exp_{b_i}$	$Exp_{b_i}$
680	5,322	5,322	5,322
851	3,302	3,302	3,302
393	2,497	2,497	2,497
26	2,320	2,320	2,320
685	1,352	1,352	1,352
684	1,349	1,349	1,349
834	1,311	1,311	1,311
833	1,306	1,306	1,306
395	983	983	983
576	822	822	822
364	782	782	782
25	593	593	593
1,080	497	497	497
438	486	486	486
194	468	468	468
819	466	466	466
215	462	462	462
5	437	437	437
8	433	433	433
686	382	382	382

Table 2 groups in eight intervals the exposure value of the 1,140 buildings in the study area. The second and third column show, in order, the total number and the percentage value of the buildings whose value of the ranking falls into the correspondent range.

**Table 2.** Grouping of the values of the exposure for the buildings in the study area.  $[a, b)$  denotes that value  $a$  belongs to the interval, while value  $b$  does not.

$Exp_{b_i}$	# $b_i$	%	Level of exposure to the landslide risk
>5,000	1	0.09	

[4,000..5,000]	0	0	
[3,000.. 4,000)	1	0.09	
[2,000.. 3,000)	2	0.18	
[1,000.. 2,000)	4	0.44	
[100.. 1,000)	56	4.9	Moderate
[1..100)	334	29.3	Low
<1	742	65.1	Null

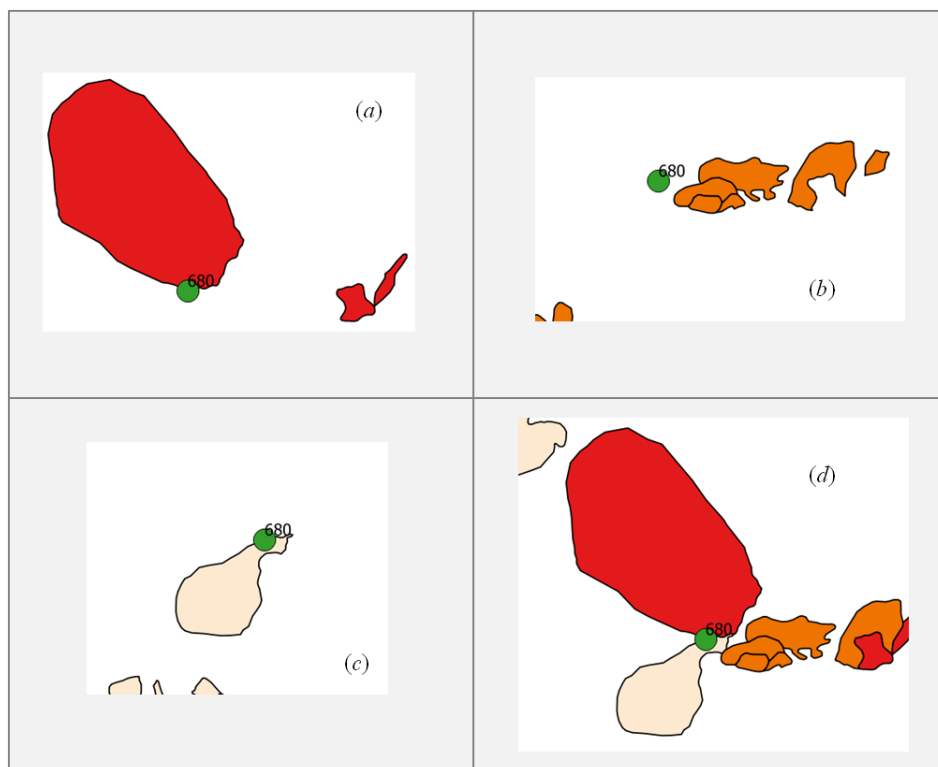
Last column of Table 2 groups the values of the exposure into four ranges: *High*, *Moderate*, *Low*, and *Null*. Those "labels" provide a qualitative classification of the level of building exposure to the landslide risk useful for officials and practitioners in mitigation to identify the buildings on which to carry out precautionary on-site checks and, if necessary, to set up a plan of actions devoted to the protection/evacuation of the buildings in response to situations of weather emergency. The four ranges were identified after a careful examination of the results of the experiments. The reasons behind such a classification are explained afterwards.

Table 1 shows that the first four buildings in the ranking have a value of the exposure much greater than the next ones. Let us now investigate what determines such high values of the exposure for those buildings.

**Table 3.** The values of the exposure for the top-4 buildings of Table 1 ( $\rho=1,000\text{m}$ ).  $Exp\_b_iS1$  denotes the value of the exposure of building  $b_i$  due to the zones of class  $S1$ . The meaning of  $Exp\_b_iS2$  and  $Exp\_b_iS3$  is analogous.

$b_i$	$Exp\_b_iS1$	$Exp\_b_iS2$	$Exp\_b_iS3$	$Exp\_b_i$
680	293	1	5,028	5,322
851	0	0	3,302	3,302
393	0	0	2,497	2,497
26	0	2,320	0	2,320

Table 3 shows that the total value of the exposure for building 680 is determined almost entirely by the value of the exposure ascribable to the danger zones of class  $S3$  (5,028). Figure 9 helps to give an explanation to those numbers.



**Figure 9.** Building 680 and the nearby danger zones in  $S3$  (a), in  $S2$  (b) and in  $S1$  (c). Map (d) shows the global scene.

The four maps show building 680 with around, in order, the zones of the class  $S3$  (Figure 9a), of class  $S2$  (Figure 9b) and of class  $S1$  (Figure 9c), while Figure 9d shows the overall scene. Figure 9a shows that building 680 is located inside a zone of the class  $S3$ . Being  $d=0$ , from Eq.2 it follows that  $Exp_{b_i} = Size \times S_{zk}$ . The high value of the exposure is determined by the considerable area of the danger zone (about  $4,700,000m^2$ ; remember that  $93,887m^2$  is the average area of all the zones in  $\mathcal{DZ}$ ) which gives rise to  $Size=50.28$ , while  $S_{zk}=100$ . According to the finding of Galli and Guzzetti (2007), that is that: "landslides whose area is around  $160,000m^2$  always produce total damage of buildings", it follows that it is appropriate to attribute a relevant weight to the exposure determined by the danger zone of Figure 9a, whose area is about 30 times higher than such a value. This finding, derived from the case study, is an indirect assessment of the effectiveness of Eq.3. Note that the two small zones that appear in the right side of Figure 9a do not take part in the calculation of the exposure since they are at about 2,000m from building 680. Analogous considerations extend to the value of the exposure determined by the zones of class  $S1$  (Figure 9c) that, as can be seen from Table 3, remains constant (293). Vice versa, in the case of the zones of class  $S2$  (Figure 9b), the value of the exposure cuts down. Similar remarks can be repeated for buildings 851, 393 and 26.

Afterwards, we discuss what determines the high values of the next four buildings (685, 684, 834 and 833) falling into the *High* range.

**Table 4.** The values of the exposure for the buildings in the positions five to eighth of Table 1 ( $\rho=1,000m$ ).

$b_i$	$Exp_{b_i,S1}$	$Exp_{b_i,S2}$	$Exp_{b_i,S3}$	$Exp_{b_i}$
685	0	5	1,347	1,352
684	0	2	1,347	1,349
834	0	1,305	6	1,311
833	0	1,303	3	1,306

Let us take into account buildings 685 and 684 together because they are distant one from the other just 156m. The (total) value of the exposure for both those buildings (Table 4) is determined by the term  $Exp_{bi\_S3}$  ascribable to the danger zone that contains both them and, only marginally, by the smaller danger zone that is far away from them of about 500m (Figure 10a). For the former zone,  $Size=13.47$  while  $Sz_k=100$ . Three danger zones of class S2 (Figure 10d) provide a contribution to the value of the exposure, but it is negligible because they are at a distance of 311m, 223m and 522m from the two school buildings.

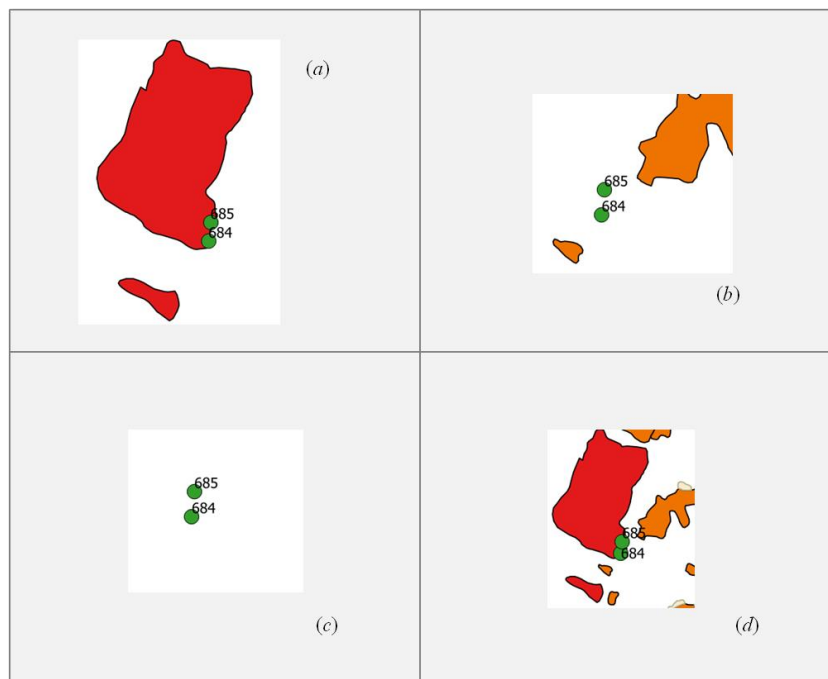


**Figure 10.** Buildings 685 and 684 and the zones close to them.

For buildings 834 and 833, too, it is possible to make a joint discussion since they are at 70m one from the other. Figure 11 shows these buildings and the danger zones close to them. The main contribution to their total value of the exposure comes from danger zones of class S2 (Table 4).  $Exp_{bi\_S2}$  is high because the two buildings fall into a danger zone (Figure 11b) of extended area (Figure 11d),  $2,400,000m^2$ , which gives rise to  $Size=25.56$ . The zone that contains the two buildings provides a contribution to the exposure equal to 1,278, plus a modest contribution from the other zones of the same class that are very close to the two buildings. It is interesting to remark that although there is a danger zone of class S3 just 325m from building 834 and 400m from building 833 (Figure 11a), it provides a negligible contribution to the total value of the exposure (6 and 3, in order). This follows from the sharp rate of decay of the value of function  $Exp_{bi,k}$  determined by the high value of the exponent ( $p=3$ ).

In summary, the analysis carried out on the eight buildings belonging to the range *High* showed that for them the high value of the exposure is determined from being contained in a danger zone either of class S3 or S2, of extension much higher than the value ( $1.6 \times 10^5 m^2$ ) indicated by Galli & Guzzetti (2007) as destructive. It follows that these eight buildings should be kept under constant control.



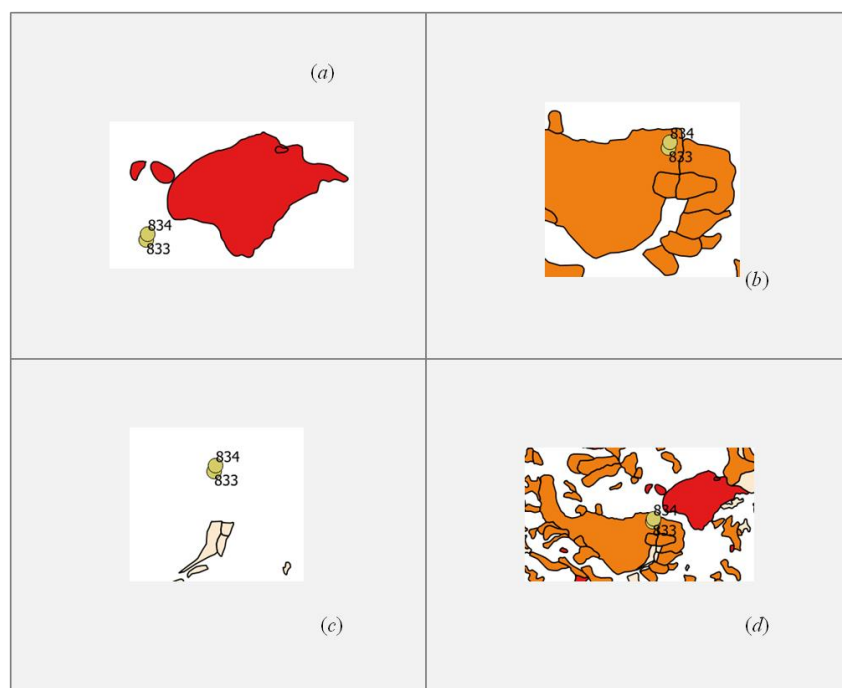


**Figure 11.** Buildings 833 and 834 and the neighbouring zones.

Now, we analyze the range [100...1000). 56 buildings belong to this group, accounting for 4.9% of the totality of the buildings involved in our study. Table 5 lists them all. Each line of this table shows, for a given building, the number of the danger zones of classes *S1*, *S2* and *S3* that are at a distance less than 1,000m from it.

The examination of the contents of Table 5, followed by feedback (via QGIS) of the geography of the territory, has allowed us to say that the ranking for the aforementioned 56 buildings is determined because one of the following situations comes true:

- $b_i$  is contained in a danger zone of class *S1* having a big *Size*, while the contribution to the value of  $Exp\_b_i$  adduced by the zones of classes *S2* and *S3* is negligible. This is the case of building 679. It is contained in a zone of  $Size=11.72$  (Figure 12a) that corresponds to a relevant area ( $1.1 \times 10^6 m^2$ ). However, the value of  $Exp\_b_i\_S1$  is low (293) due to the small value of  $S_{zk}$  (25);
- $b_i$  is contained in a danger zone of class *S2* having a big *Size*, while the contribution to the value of  $Exp\_b_i$  adduced by the zones of classes *S1* and *S3* is negligible. This is the case of building 576 (Figure 12b). It is contained in a zone of  $Size=16$  that corresponds to a very relevant area ( $4.7 \times 10^6 m^2$ ). The value of  $Exp\_b_i\_S2$  is equal to 800 (remember that for the danger zones of class *S2*,  $S_{zk}=50$ );
- $b_i$  is not contained in any danger zone of the three classes, but it is "nearly in touch" with the boundary of a zone of class *S3* having big *Size*. Moreover, the contribution adduced by the zones of the classes *S1* and *S2* is negligible. This is the case of building 364 (Figure 12c);
- $b_i$  is not contained in any danger zone of the classes *S1*, *S2*, or *S3*, but there are many danger zones very close to it belonging to one or more of those three classes. This is the case, for instance, of building 25 (Figure 12d), as well as of buildings 438, 215, 195, 20, 1,098, 699, 216, 289, 51, etc.

**Table 5.** The ranking of the buildings in the range [100..1000). #*S1* (#*S2*, #*S3*) denotes the number of  $z_k$  of class *S1* (*S2*, *S3*) at distance less than 1,000m from  $b_i$ .

Ranking	$b_i$	# <i>S1</i>	$Exp\_b_i\_S1$	# <i>S2</i>	$Exp\_b_i\_S2$	# <i>S3</i>	$Exp\_b_i\_S3$	$Exp\_b_i$
---------	-------	-------------	----------------	-------------	----------------	-------------	----------------	------------

9	395	0	0	7	1	2	982	983
10	576	2	0	15	822	0	0	822
11	364	1	0	0	0	1	782	782
12	25	0	0	7	593	1	0	593
13	1,080	3	0	4	0	6	497	497
14	438	1	0	3	485	1	1	486
15	194	1	0	4	0	6	468	468
16	819	5	2	7	3	1	461	466
17	215	1	0	8	1	3	461	462
18	5	5	6	13	1	1	430	437
19	8	6	2	11	0	1	430	433
20	686	1	0	4	9	1	373	382
21	195	1	0	5	0	6	369	369
22	865	0	0	10	0	1	353	353
23	20	1	0	11	2	6	323	324
24	1,098	3	0	7	0	5	311	311
25	699	1	0	14	0	6	301	301
26	679	1	293	2	0	1	5	298
27	216	1	0	8	0	3	270	270
28	289	10	0	10	249	5	0	250
29	51	4	0	11	245	6	0	246
30	461	1	0	6	1	8	239	240
31	134	0	0	12	230	4	0	230
32	23	1	0	6	5	4	216	221
33	435	1	0	5	1	12	219	220
34	133	0	0	10	191	7	0	191
35	167	1	0	7	0	9	188	188
36	266	12	2	17	27	20	156	185
37	114	5	0	7	183	3	0	183
38	168	1	0	7	0	10	182	182
39	303	0	0	16	174	2	0	174
40	1,126	2	0	1	0	6	171	172
41	1,037	3	0	10	171	6	0	171
42	801	3	165	2	0	2	0	165
43	1,082	3	0	11	7	7	156	162
44	110	1	0	12	0	10	161	162
45	107	0	0	6	9	1	147	157
46	288	9	0	8	153	7	2	155
47	6	6	21	12	0	1	123	145
48	153	1	0	11	11	8	132	143
49	1,135	3	0	5	1	5	141	142
50	939	0	0	7	7	1	131	138
51	302	2	0	7	0	4	133	133
52	152	1	0	10	1	8	132	132
53	206	3	0	11	6	5	120	126
54	407	2	0	8	115	8	11	126
55	165	6	1	2	120	4	5	125
56	324	2	0	11	117	0	0	117
57	938	0	0	7	4	1	109	114
58	695	4	3	14	1	5	105	109
59	444	4	0	10	105	1	0	105
60	39	1	0	8	11	21	94	105
61	845	0	0	0	0	1	103	103
62	176	3	0	12	98	3	5	103
63	124	3	0	11	6	4	96	103
64	211	3	0	12	3	10	98	101

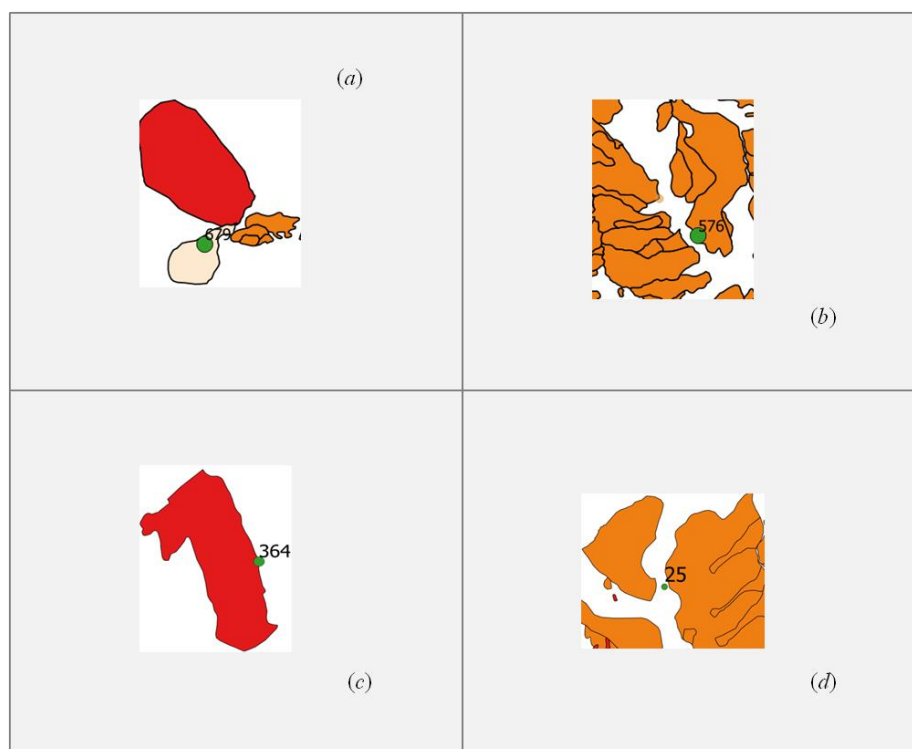


**Figure 12.** Some buildings in the range *Moderate* of Table 2 and the zones surrounding them.

About the buildings with exposure in the range [1...100) (94.4% of the total, i.e., 1,076 buildings), we observed the following. None of them falls into some danger zone of the classes *S1*, *S2* or *S3*; moreover, in the cases where the buildings are next to some danger zone these latter have *Size* very low, vice versa if it happens that *Size* is not very low, then the danger zone nearest to the building is at a distance of several hundred meters from it. The conclusion is that the buildings belonging to the *Low* range (Table 2) are not in a remarkable danger, therefore for them is not required an on-site inspection.

The potential hazard fades entirely for buildings with exposure less than 1. They, too, can be ignored.

### 3.1 Notes of caution

The ranking returned by the proposed method is affected by the completeness and the quality of the data about the danger zones. Completeness and quality of the input data are critical issues reported in almost all studies of the sector, e.g. (SafeLand, 2011), (Blahut et al., 2012), (Varazanashvili et al., 2012), (Erener and Düzgün, 2013).

Downstream of the acquisition of the ranking returned by our method, it will be necessary to carry out on-site inspections for the buildings in the *Moderate* range that do not fall in danger zones of either classes *S3* or *S2*. This because the method may return *false positives* due to the fact that it, in its current version, does not take into account the terrain elevation.

Our method is *simple* and this increases the need to validate it. In order to carry out such a task it is necessary to have a landslide dataset repository about the Abruzzo region, as that prepared, for example, by (Salvati et al., 2009). Their catalogue lists information about 224 sites inside the Umbria region (central Italy) where buildings and other structures were damaged by landslides. Unfortunately, for the Abruzzo region such a dataset is not available (Trigila et al., 2010).

## 4. CONCLUSIONS AND FUTURE WORK

We have proposed a simple method suitable to rank the buildings present over a developed, large territory based on their degree of exposure to the landslide hazard. Similarly to other studies appeared in the literature, e.g. (Galli and Guzzetti, 2007), the method has a heuristic basis: we conjecture that the value of the exposure of a building depends *only* on the neighboring susceptibility zones.

The method has been tested on 1,140 buildings hosting public schools in the Abruzzo Region (central Italy). The safety of this category of buildings is currently one of the most important national emergency target of the Civil Protection department.

The case study was carried out by downloading data from public sites, namely that of the Ministry of the Environment (data about the school buildings) and that of the Abruzzo region (an incomplete landslide inventory that represents a rough approximation of set  $\mathcal{DZ}$ ). Our method is applicable in the same way, and obviously with better results, if the shapefiles corresponding to the *landslide susceptibility maps* are available. Those data/maps are well-known in the literature, e.g. (Guzzetti et al., 2006), but rarely available to the public administrators.

Our assessment scheme, implemented in a GIS environment, produces in few minutes and at low cost a huge amount of data. The results give an overview over the reference geographic area and, thanks to the ranking, it is easy to select the buildings on which the investment of public money will yield the highest protective effect for humans and assets. We hope that the suggested method could be an inspiration for other communities all over the world.

The results of the case study allow us to state that the buildings to be monitored primarily, through on-site inspections, are those belonging to the *High* range. They are just 8 out of 1,140. Then, the focus can be shifted to the buildings in the *Moderate* range (56 out of 1,140, a mere 4.9% of the totality of the buildings present in the study area). These numbers proof that the aim of our study has been centered, i.e. to provide the responsible for land management with a tool suitable to detect easily the top-N buildings on which they have to concentrate the attention as well as the human and financial resources. The importance of this result has been highlighted in Sec.1, therefore will not be repeated.

Our proposal is within the context of the preventive monitoring of the territory and of the assets on it. This justifies a characteristic of the proposed method, namely that it is inclined to return *false positives* (i.e., false alarms), to avoid *false negatives* (i.e. the eventuality of not including in the top positions of the ranking buildings that could be exposed to a high level of landslide risk). The correct way to use the ranking is to make on-site inspections in order to detect the buildings mistakenly inserted in the top positions of the ranking (if any). The happy note is that the number of inspections to be done is small in comparison with the total number of buildings present in the study area.

In summary, the outcome of our method may be helpful from three points of view:

- a) to be used in combination with other analysis techniques targeted to the vulnerability assessment;
- b) to promptly identify the buildings actually exposed to a high degree of landslide hazard, among *all* that are located inside an area that can be affected by a severe natural event;
- c) to set up a plan of actions devoted to the protection/evacuation of buildings in response to situations of weather emergency (Hubbard et al., 2014).

This paper constitutes the first step in the direction of making available a method, to be implemented with GIS software technologies, for ranking the buildings present over a developed, large territory based on their degree of exposure to the landslide hazard. The

distance between buildings and the danger zones, and the area of the latter determine the final ranking of the former. The next step will be devoted to embed into the proposed method the elevation of the terrain. In this way, it will be possible to cut off from the ranking the false positives that the current version of the method is unable to detect.

## REFERENCES

- Blahut, J., Poretti, I., De Amicis, M., Sterlacchini, S. 2012. Database of geo-hydrological disasters for civil protection purposes. *Natural Hazards* 60:1065–1083, DOI 10.1007/s11069-011-9893-6.
- Brabb, E.E. 1984. Innovative approach to landslide hazard and risk mapping. Proceedings of the 4th International Symposium on Landslides, Toronto, Vol. 1, 307–324.
- Brabb, E.E., Harrod, B.L. (Eds.), 1989. *Landslides: extent and economic significance*. Balkema Publisher, Rotterdam. 385 pp.
- Dai, F.C., Lee, C.F. and Ngai, Y.Y. 2002. Landslide risk assessment and management: an overview. *Engineering Geology* 64, 65–87.
- Di Felice, P., et al. 2014. A proposal to expand the community of users able to process historical rainfall data by means of the today available open source libraries. *Journal of Computing and Information Technology - CIT* 22, 2, 1–19, doi:10.2498/cit.1002345.
- Di Felice, P. 2015. Assessing the Impact of the Geographical Scale on the Maximum Distance Error: A Preliminary Step for Quality of Life Studies. *European Journal of Geography*, 6:3, 69–78.
- Erener, A., Düzgün, H.S.B. 2013. A regional scale quantitative risk assessment for landslides: case of Kumluca watershed in Bartın, Turkey. *Landslides*, 10:55–73, DOI 10.1007/s10346-012-0317-9.
- Fell, R., et al. 2008. Guidelines for landslide susceptibility, hazard and risk zoning for land-use planning, *Engineering Geology*, 102:99–111.
- Fuchs S., Kuhlicke C., Meyer V. 2011. Vulnerability to natural hazards. The challenge of integration. *Natural Hazards*, 58:609–619.
- Fuchs, S., Birkmann, J., Glade, T. 2012. Vulnerability assessment in natural hazard and risk analysis: current approaches and future challenges. *Natural Hazards*, 64:1969–1975. DOI 10.1007/s11069-012-0352-9.
- Galli, M., and Guzzetti, F. 2007. Landslide vulnerability criteria: a case study from umbria, central Italy. *Environmental Management*, 40:649–664, DOI 10.1007/s00267-006-0325-4.
- Guzzetti, F., Stark, C.P., Salvati, P. 2005. Evaluation of flood and landslide risk to the population of Italy. *Environmental Management*, 36:1, 15–36. DOI: 10.1007/s00267-003-0257-1.
- Guzzetti, F., et al. 2006. Estimating the quality of landslide susceptibility models, *Geomorphology*, 81:166–184.
- Hervás, J. 2013. Encyclopedia of Natural Hazards, Encyclopedia of Earth Sciences Series, pp 610-611. Editor P. T. Bobrowsky, [http://link.springer.com/referenceworkentry/10.1007%2F978-1-4020-4399-4\\_214](http://link.springer.com/referenceworkentry/10.1007%2F978-1-4020-4399-4_214).
- Hubbard, S., Stewart, K., and Fan, J. 2014. Modeling spatiotemporal patterns of building vulnerability and content evacuations before a riverine flood disaster. *Applied Geography*, 52,172-181.
- Jaedicke, C., et al. 2014. Identification of landslide hazard and risk ‘hotspots’ in Europe. *Bulletin of Engineering Geology and the Environment*, 73:325–339. DOI: 10.1007/s10064-013-0541-0.

- Jongman, B., et al. 2012. Comparative flood damage model assessment: towards a European approach. *Natural Hazards and Earth System Sciences*, 12, 3733–3752. [www.nat-hazards-earth-syst-sci.net/12/3733/2012/](http://www.nat-hazards-earth-syst-sci.net/12/3733/2012/). DOI: 10.5194/nhess-12-3733-2012.
- Liu, M., Lo, S. M., Hu, B. Q., and Zhao, C. M. 2009. On the use of fuzzy synthetic evaluation and optimal classification for computing fire risk ranking of buildings. *Neural Computing & Applications*, 18:643–652. DOI: 10.1007/s00521-009-0244-4.
- Magliulo, P., Di Lisio, A., and Russo, F. 2009. Comparison of GIS-based methodologies for the landslide susceptibility assessment, *Geoinformatica*, 13:253–265. DOI 10.1007/s10707-008-0063-2
- Mandal, S. and Maiti, R., (2013), Assessing the triggering rainfall-induced landslip events in the shivkhola watershed of darjiling himalaya, west bengal. *European Journal of Geography*, 4:3, 21–37.
- Mazzorana, B., et al. 2014. A physical approach on flood risk vulnerability of buildings. *Hydrology and Earth System Science*, 18, 3817–3836. [www.hydrology-earth-syst-sci.net/18/3817/2014/](http://www.hydrology-earth-syst-sci.net/18/3817/2014/). DOI: 10.5194/hess-18-3817-2014.
- Peri, G., and Rizzo, G. 2012. The overall classification of residential buildings: Possible role of tourist EU Ecolabel award scheme. *Building and Environment*, 56, 151–161.
- Photis, Y.N. 2012. Redefinition of the Greek Electoral Districts through the Application of a Region-Building Algorithm, *European Journal of Geography*, 3:2, 72–83; [http://www.eurogeographyjournal.eu/articles/EJG01206\\_photis.pdf](http://www.eurogeographyjournal.eu/articles/EJG01206_photis.pdf).
- Rawat, P.K., Tiwari, P.C., Pant, C.C. 2012. Geo-hydrological database modeling for integrated multiple hazards and risk assessment in Lesser Himalaya: a GIS-based case study. *Natural Hazards*, 62:1233–1260. DOI 10.1007/s11069-012-0144-2.
- SafeLand, 2011. Guidelines for landslide susceptibility, hazard and risk assessment and zoning. Deliverable D2.4 of the SafeLand research project, 7th EU Framework Programme. (<http://www.safeland-fp7.eu/Pages/SafeLand.aspx>).
- Salvati, P., et al. 2009. A WebGIS for the dissemination of information on historical landslides and floods in Umbria, Italy. *Geoinformatica*, 13:305–322. DOI 10.1007/s10707-008-0072-1
- Tobler, W. 1970. A computer movie simulating urban growth in the detroit region. *Economic Geography*, 46, 234–240.
- Trigila, A., Iadanza, C., and Spizzichino, D. 2010. Quality assessment of the Italian landslide inventory using GIS processing. *Landslides*, 7:455–470, DOI 10.1007/s10346-010-0213-0.
- Varazanashvili, O., et al. 2012. Vulnerability, hazards and multiple risk assessment for Georgia. *Natural Hazards*, 64:2021–2056, DOI 10.1007/s11069-012-0374-3.
- Varnes, D.J., et al. 1984. Landslide hazard zonation: a review of principles and practice. *Natural Hazards*, Vol.3. United Nations Educational Scientific and Cultural Organization.